Modelling and design of a small scale solar tracking system; Application to a green house model

Ph. DONDON (1)- L. MIRON (2)
(1)Université de Bordeaux, IPB, UMR 5218, Av Dr A. Schweitzer 33405 Talence, France.
(2) AFA, St. Mihai VITEAZUL, nr. 160, 500187 Brasov, Romania
Philippe.Dondon@enseirb-matmeca.fr

Abstract: Power generation is one of the challenges in Sustainable Development. For example, well known sun tracking systems allows improvement of solar panel power ratio. In order to illustrate this concept, this paper presents a simplified and didactical small scale system for pedagogical application and sensitizing actions. Principle of tracking is described. A mixed SPICE modelling of the system, including geometrical, optical, electronic linear and non linear aspects is built. Simulations results are analyzed. Electronic analogue design is detailed, experimental test are presented before conclusion. This small scale solar tracking system is now installed in a green house model.

Key words: Sun tracking, Mixed SPICE modelling, Analogue design, Sustainable development

1. Introduction

1.1 Small scale house project

Three years were necessary for ENSEIRB-MATMECA school with some academic partners, to design a functional realistic small scale house, built in genuine materials. It was completed successfully within the framework of an innovative sustainable development project. The building (with true materials) of small scale house itself is finished. It required more than 1500 hours of work [1]. Figure 1 shows a picture of the finished modular scale model (1/20 scale).

Figure 1: View of house and surroundings.

The model will be used as:

- Demonstrator (sustainable development exhibition in town halls or local sustainable development events)
- Pedagogical support for practical lessons and electronic projects, for sensitizing engineering students to green power management, power saving and low power electronic in first and 2nd year study.

1.2 Study framework

To make our green house model more realists, didactical and functional, we designed several accessories and their electronic control circuits, for example:

- A low voltage LED lighting for the terrace and house supplied by a roof solar panel and battery cells.
- An hydrogen fuel stack who supplies a fan for house "air conditioned" system (i.e. scaled Canadian well under the house),
- A solar dish with temperature measurement,
- A solar tower and its performance measurement system,
- An electrical heater circuit house and its temperature control…

The present paper focuses on the modelling and design of the small scale simplified solar tracking system for a solar panel installed in the house garden (Cf. figure1).

1.3 Solar tracking

Professional and industrial true systems are generally based processor board in which the position of the sun is generally tabulated (from astronomical data), all over the year. Position of the solar panel follows the programmed law on two axes, taking into account the sun ray optical diffraction or refraction into atmosphere.

A real solar tracking system can improve the electricity production of a solar panel [2], [3] up to 27 % for a double axis tracker and 23 % for a single axis tracker.

2. Sun tracking circuit

2.1 Generalities

The didactical proposed circuit is obviously a simplified version of a true system [4]. However, it is enough complex for a didactical approach of tracking and to illustrate analogue feed back theoretical courses given in our electronic engineering school. More generally, this study is an opportunity to sensitize the students to sustainable development.

2.2 Tracking system principles and schematic

As our "green house" is used for in-door demonstration, a halogen spot light is used to "replace" the sun light.

The design is based on a simple analogue system with one rotation axis control (horizontal plan). Figure 2 shows the sun tracking block diagram.

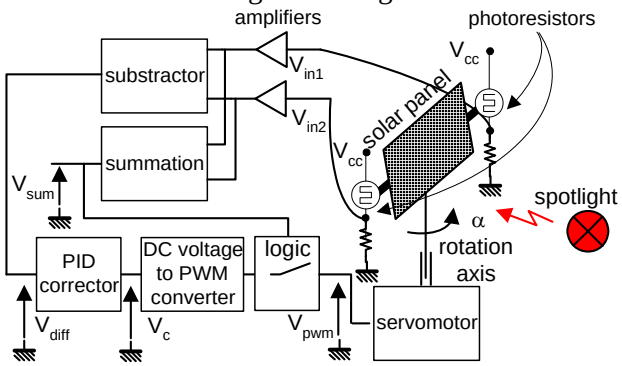

Figure 2: Sun tracking system block diagram

It works as follows: two light sensors LDR1 and LDR2 (LDR: Light Dependant Resistors,), located on left and right side of the panel receive the "sun" light.

When the solar panel is well align in "sun" direction, the received left and right lights flux L1 and L2 are equal. When it is not, one of the two LDR receives more flux than the other, and feed back loop moves the servo motor into the right direction to cancel the voltage difference V_{diff} "left minus right" signals (Cf. figure 3).

Since the servomotor is a classical hobbyist servo, a DC to PWM converter is required: indeed, the rotation angle of a servomotor is proportional to a control signal pulse width V_{pwm} (1ms to 2ms for a 180° range).

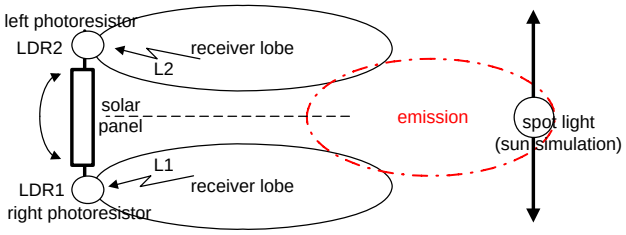

Figure 3: Solar panel alignment

Summing the two sensors voltage allows the system to distinguish dark and sunny situation. Thus, during "night" the servo control is deactivated to minimize power consumption. The system is supplied by a single supply voltage +5V.

2.3 Modelling interest

The principle explained in §2.2 is well known since a long time. Similar applications using infrared diodes or ultrasonic sensors instead of LDR are described in [5], [6], [7], [8]. And practical designs are given in common literature. However, between black box and final electronic design, a medium level modelling is rarely found. The paragraph 3 of this study aims to present a medium complex modelling to make the link between a general synoptic and a basic electronic design.

3. Tracking system modelling

3.1 Generalities

Modelling is not easy because the whole system consists of several heterogeneous parts. Modelling of the whole system must take into account electronic behaviour (Electronic circuits, non linear sensors (LDR1 and LDR2), servomotor), but also optical and geometrical aspects, due to the movement of the spot light (simulating the sun). That requires a global approach. Among several possibilities, we propose hereafter, the building of an "easy to use" mixed SPICE modelling which do not requires specific competencies.

Figure 4 shows the identified blocks of the whole system and figure 5 gives the corresponding geometrical angles vs. absolute compass points and vs. perpendicular bisector of LDR1, LDR2 segment. In order to simplify the approach, the range of rotation angle -i.e. 180° for a classical servomotor- is supposed covering a sweep from East to West.

Each block has to be modelled by a transfer function. Thus, a global and equivalent SPICE modelling can be build.

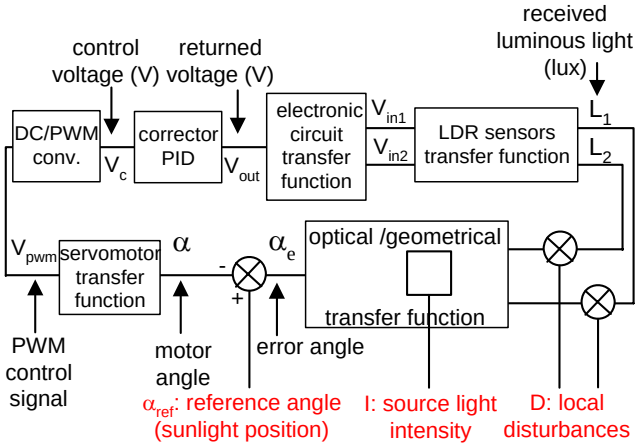

Figure 4: System identification

L_1, L_2 represents the received light (in Lux) on each LDR, α_{ref} the sun angular position, α_e the error angle α the angle given by the servo motor.

- α_{ref} is the main input of the feed back system.
- Source light intensity input (I) can be seen as a parasitic input which represents fluctuation of source intensity (fog, sky partially cloudy, etc).
- Local disturbances input (D) represent disturbances that can occur individually, on each LDR optical way. (LDR partially hidden by an object passing over, etc).

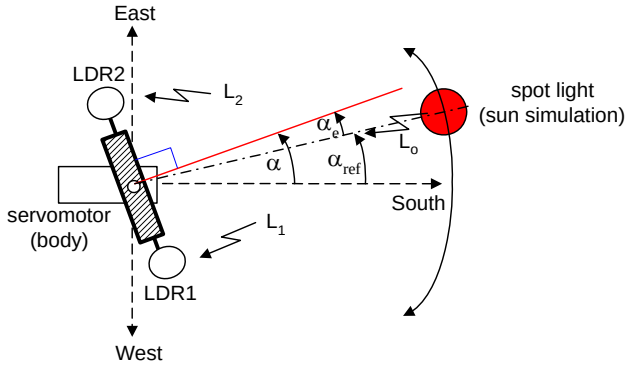

Figure 5: Reference angles (top view)

3.2 Modelling of received luminous light

3.2.1 Optical/ Geometrical modelling

This aim of this simplified modelling is to obtain the relation between received light L_1 and L_2 (in lux) on each LDR sensors and the incidence angle α_e of the spotlight.

Assuming that spotlight is a punctual source, distance to spotlight D is greatly bigger than *l*, (distance between LDR sensors), all angles in the figure 6 can be considered as small. LDR surfaces are supposed equal to $S_o = \pi.d^2/4$ and $\Theta_o = \text{arctg}\,(l/2D)$.

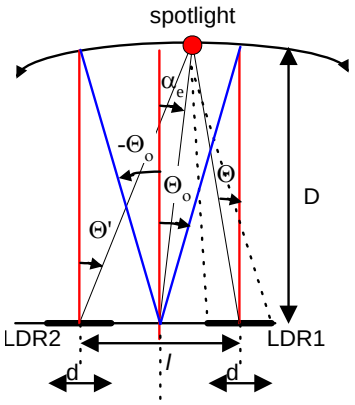

Figure 6: Geometrical drawing

Received light varies with the angles of incidence Θ, Θ' [9]:

$$L_1 = L_0 \cos \Theta$$
$$L_2 = L_0 \cos \Theta'$$

with: $L_0 = I. / D^2$, where I is the light intensity of the source (in Candela).

For small variations around the medium position:

$$\Theta' \approx \alpha e + \Theta_o$$
$$\Theta \approx \Theta_o - \alpha e$$

It yields:

$$L_1 = L_0 \cos (\Theta_o - \alpha e)$$
$$L_2 = L_0 \cos (\alpha e + \Theta_o)$$

When $\alpha_e = 0$, (spotlight centered), $L_1 = L_2$.

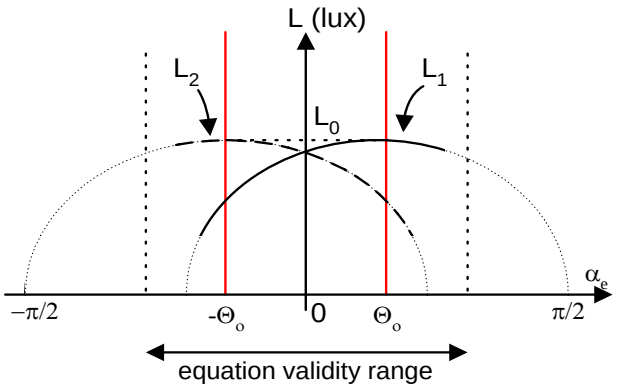

Figure 7: Received light L_1 and L_2 vs. angle α_e

3.2.2 Received light SPICE modelling

From these equations, we can build equivalent SPICE modelling, using ABM library elements.

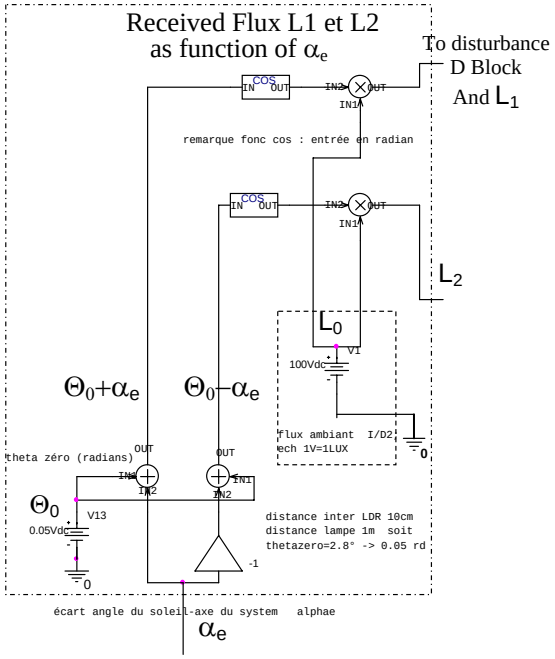

Figure 8: SPICE received light modelling

3.3 Modelling of LDR sensors

Due to manufacturing process, LDR behaviour's varies a lot [10], [11]. Thus, modelling must be extracted from experiments.

3.3.1 LDR characterisation

For a correct and symmetric operation of the tracking system, the two LDR sensors were sorted and a fine selection of two matched LDR was done.

Static characterisation [12], [13] is done with the simple test equipment represented in figure 9.

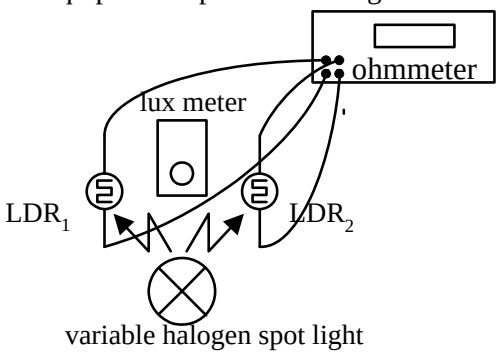

Figure 9: LDR static characterisation test bench

A selected set of LDR were tested as indicated hereafter: The LDR VT90N2 equivalent are exposed to a variable intensity with an halogen spot light. Lux meter ROline -1332 and a digital ohmmeter are used for the characterisation (cf. figure 4).

Figure 10 shows the experimental results.

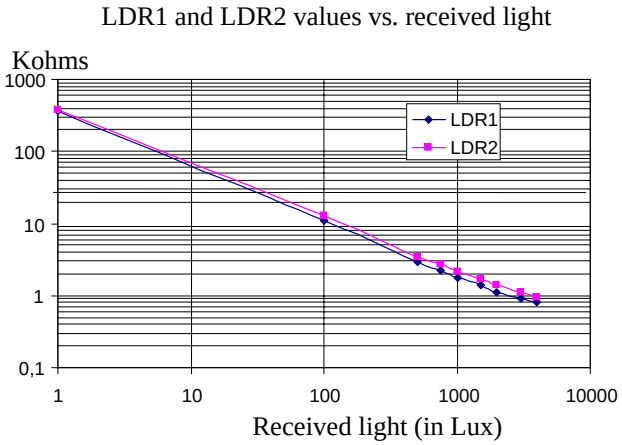

Figure 10: Static LDR characterisation

The dynamic response is obtained by submitting the LDR -inserted in a resistor bridge- to a light pulse dark to bright and bright to dark: Rise time dark to bright is around 100ms while fall time bright to dark is around 900ms. Rise time and fall time are very different.

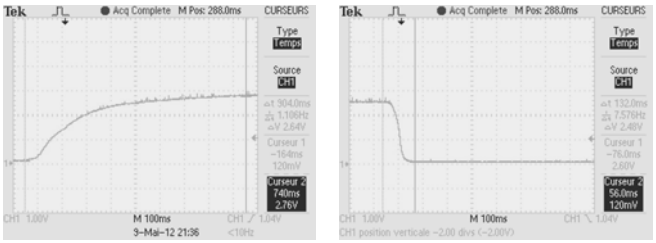

Figure 11: Dynamic LDR characterisation

But it is an extreme case because source light intensity can not vary instantaneously. Thus, we will take an average value of 200ms. For various reasons, LDR response time is included in servomotor modelling (See §3.5.2).

3.3.2 Modelling extraction

Our commercial LDRs samples vary over 3 decades as a non integer power of the received light (i.e. from $L^{-0.5}$ to $L^{-0.7}$). Among tested LDRs, we selected the ones who have the closest behaviour, thus:

$$LDR(\Omega) = k.\frac{1}{L^{0.7}}$$

3.3.3 SPICE equivalent Modelling

ABM library "PWR" Spice element, a "Voltage Controlled Resistance", and a perfect gain element are used for modelling of LDR. Figure 12 shows the LDR modelling inserted in a resistor bridge R3, R4.

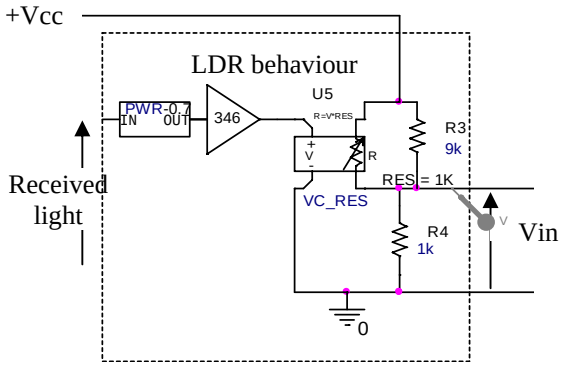

Figure 12: LDR (1, 2) SPICE modelling

3.4 Modelling of electronic circuits

3.4.1 Subtraction function

We have to make subtraction of the two voltages delivered by the two LDR sensors.

3.4.2 SPICE equivalent Modelling

The spice simulated circuit corresponds directly to the used electronic basic circuit, with 3 OP AMP.

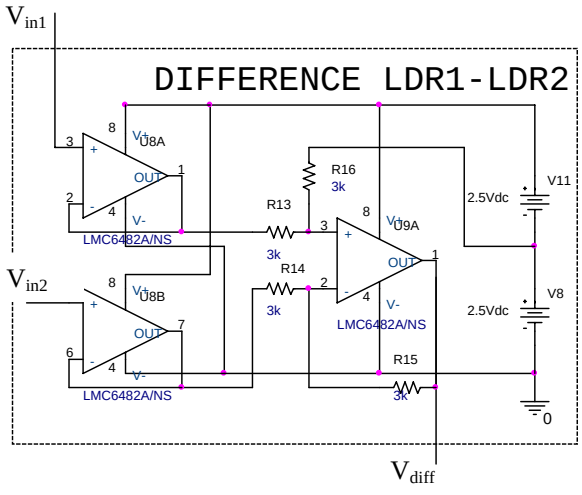

Figure 13: circuits SPICE modelling

3.5 Modelling of servomotor

3.5.1 Servomotor selection

A classical Hobbyist servo Parallax or equivalent, medium size is used (Cf. figure 14). Supply voltage is +5V. Control signal V_{pwm} is a PWM periodic signal: period 20ms, pulse width 1ms to 2ms for an angle range of 180°. Maximum rotation speed is 60°/0.15s.

Figure 14: Servomotor

3.5.2 Servomotor and DC/PWM converter modelling

When Vc control voltage varies from 0V to 5V, the DC to PWM converter generates a V_{pwm} signal with a variable pulse width from 1ms to 2ms. The corresponding α angle varies proportionally from -90° to +90°. Thus DC to PWM converter is modelled by a simple coefficient of 0.62 rd/V.

The dynamic behaviour of the system has been extracted by experimental measurements that included LDR and servo response. Figure 15 gives the equivalent modelling for DC to PWM converter and servomotor. Saturation block represents the angular speed limit (60°/0.15s).

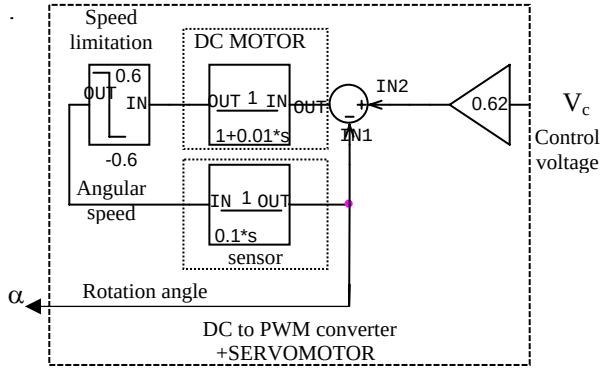

Figure 15: DC/PMW and Servo motor SPICE modelling

3.6 Local disturbance (D) modelling

An optional disturbance inputs (D)can be inserted between outputs of the "received light modelling" block and "LDR modelling" block for simulations presented in §4.2.3.

As the two LDR ways are symmetrical, the disturbance input can be added indifferently on one or the other LDR optical way of the global modelling. Here, we choose LDR1.

For these specific analysis, an extra SPICE element Voltage controlled Switch (VCSW) is used. Indeed, such disturbance does not act as an additional signal in the loop. When disturbance occurs, received L_1 light is suddenly reduced and the LDR1 feed back loop way is momentously "broken" while the feed back loop on LDR2 still operates normally. It leads to the following modelling given in figure 9.

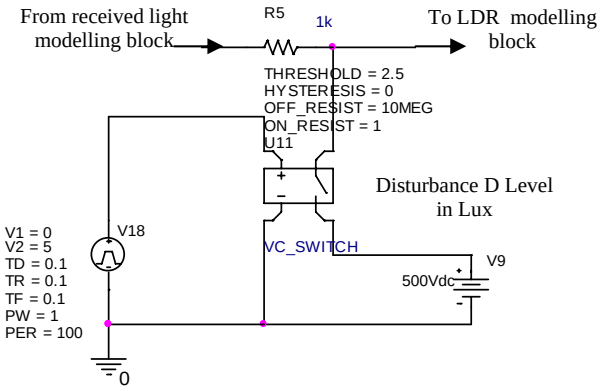

Figure 16: Disturbance input modelling

3.7 Tracking system global modelling

Once each block modelled, they can be merged in a global equivalent schematic as indicated in figure 17. Since SPICE stimuli are obviously in Volt and Amp, correspondence scales have been defined as follows:
1Vdc->1 Lux for light flux
1Vdc -> 1 rd for angles

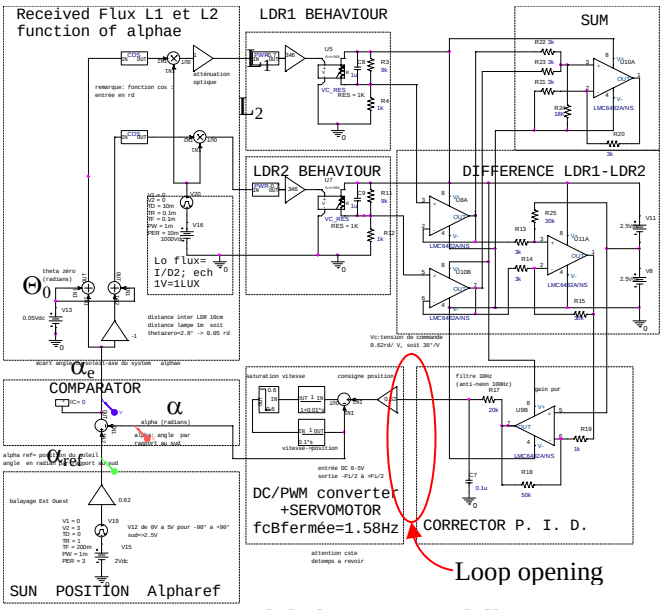

Figure 17: Global SPICE modelling

3.8 Loop correction

The loop is a natural 2nd loop order (LDR +servo). Loop correction (simple proportional correction) has to be adjusted taking into account two electronic constraints:
a) The response of photo resistors to the luminosity is non linear. Consequently, the open loop gain change with absolute light level. To make PID correction as easy as possible, corrector has been designed for the worst case.
b) As we do not need a high precision alignment with sun direction, we chose to reduce the open loop gain at a minimum acceptable value to avoid oscillations at any conditions. In any cases, the alignment angle accuracy is better than 5°, which is enough to show the spot light tracking operation.

4. SPICE simulations

Among numerous simulations, we give hereafter the most significant ones.
As SPICE works obviously in Volt and Amp, horizontal and vertical scales of the simulated response curves are converted (if necessary) in radians angles and Lux before display, for better understanding.

Figure 18 gives the simulated static response of the LDR. (has to be compared with figure 10).

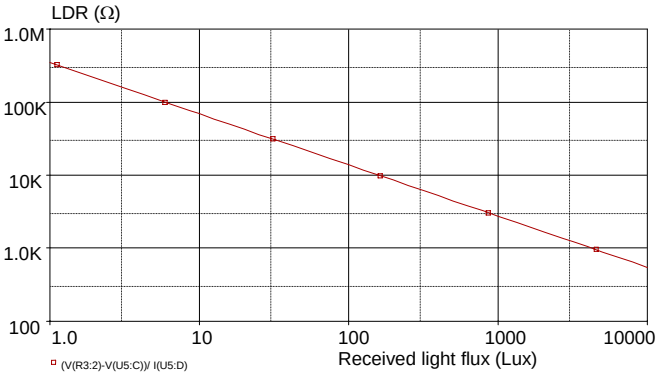

Figure 18: LDR spice simulation

4.1 Open loop simulations

Figure 19 gives the static behaviour in open loop, with a simple proportional correction, when submitting the system to a DC sweep of α angle from -90° to +90° (i.e. full rotation from East to West) when the spot light is south position (α_{ref} locked at 0°).
Upper curves shows L_1 and L_2 lights flux. L_1, L_2 reach their maximum values L_0 (here =1000 lux) when the spotlight is exactly in front of them (Respectively $\alpha_e = \Theta_o$ and $\alpha_e = -\Theta_o$). And they tend toward 0 when α reaches ± 90° (Sunset or sunrise situation).

Lower curve shows the difference signal V_{diff} centered on Vsupply/2 (i.e. $V_{cc}/2$= 2.5V). It is a classical "S" curve: when the light source is centered, V_{diff} is centered on 2.5V. When the source light is shifted above LDR2, V_{diff} becomes greater than $V_{cc}/2$. When the source light is shifted above LDR1, V_{diff} becomes smaller than $V_{cc}/2$. V_{diff} is thus well suitable for feed back control. When α reaches ± 90° (Sunset or sunrise situation), L1 and L2 tend toward 0, thus V_{diff} return to Vcc/2.

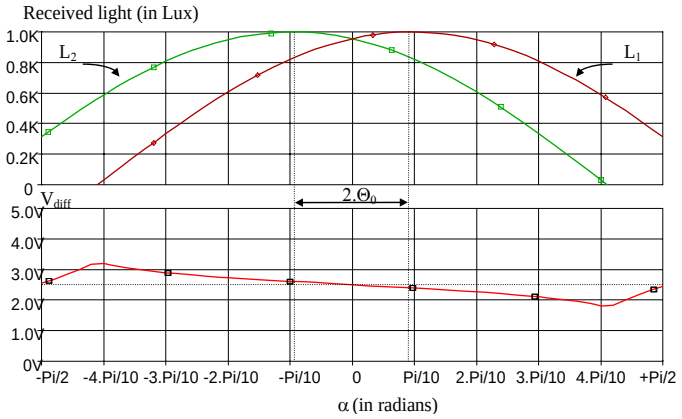

Figure 19: Open loop simulation (DC sweep)

Figure 20 shows the AC open loop response. Small variations of α (<< Θ_0) are applied around the mid position (south).The open loop response varies like a 2nd order circuit. Because of system nonlinearity, the static gain depends obviously on L_0 light flux value. Here, a parametric sweep shows curves for L_0 = 10, 100, 1000 and 10000 lux. Static error and stability are obviously impacted (see § 4.2 and 9).

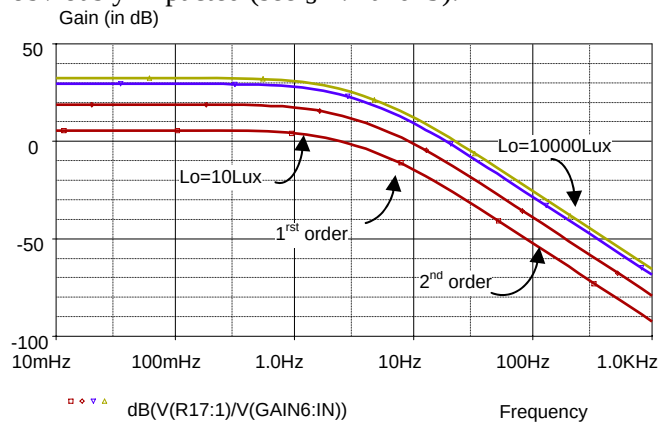

Figure 20: Open loop simulation (AC)

4.2 Closed loop Simulations

4.2.1 Response to setup angle value

A slow transient ramp is applied on α_{ref} input to simulate a full rotation from East to West. Figure 21 shows a good tracking since error angle α_e remains close to zero (less than ±2.5°C) during all the simulated rotation.

Upper curve: zoomed error angle α_e vs. reference angle α_{ref}.

Lower curves: reference angle α_{ref}, servomotor angle α vs. reference angle α_{ref} .

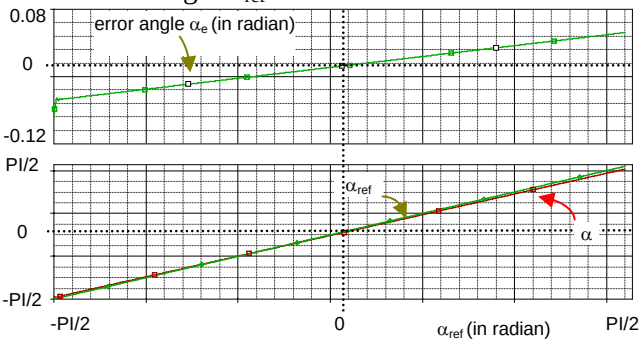

Figure 21: Closed loop transient response and residual static error α_e

Since there is no integration in the feed back loop, error angle is proportional to the "DC to PWM" converter input control voltage V_c, and thus to reference angle.

Figure 22 shows the AC closed loop response. Gain in bandwidth is close to 1, according to the feed back theory.

A parametric sweep for L_0 = 10, 100, 1000 and 10000 lux highlights possible stability problem at high source intensity level. However, for an indoor use with a classical halogen spotlight, light intensity does not exceed 1000 lux: stability is ensured.

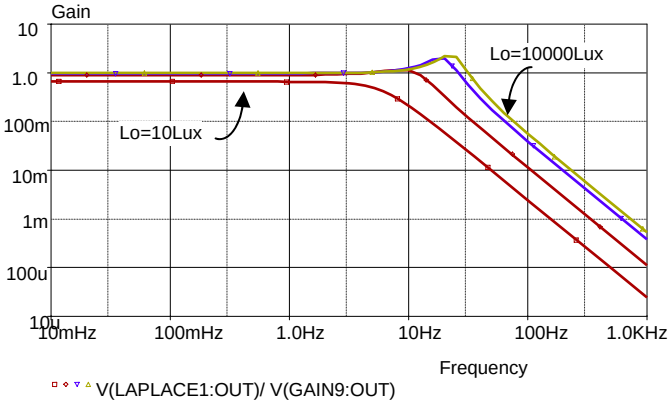

Figure 22: Closed loop AC response

4.2.2 Response to light source intensity fluctuations

As the light source is located far from the LDR sensors, fluctuations of source intensity (input I) affect identically LDR1 and LDR2: They can be considered like a common mode and parasitic for the loop. Figure 23 shows the AC loop response to 10% fluctuations

the source (100 Lux around de 1000 Lux), α_e varies less than 1mrd over the bandwidth and decrease after. These parasitic fluctuations are well rejected. That leads to an almost total insensitivity of the system while LDR sensors are perfectly matched.
Indeed, mismatching between the two LDR sensors could seriously affect the loop behaviour (see § 9).

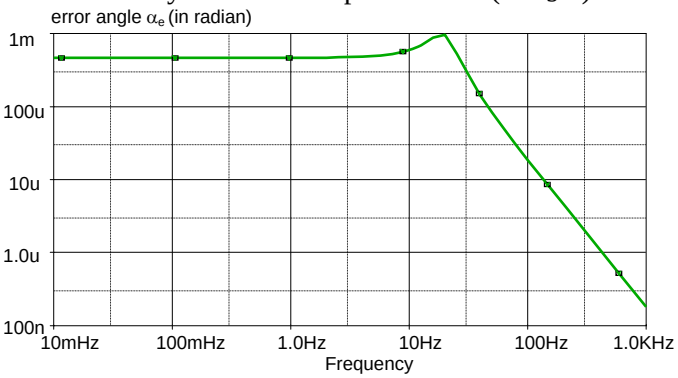

Figure 23: Closed loop response to fluctuation of source intensity (I input).

4.2.3 Response to local LDR disturbance

This last simulated situation corresponds to an object passing above one LDR during a few second. Thus, one of the LDR looks like it was momentously "blind". Due to the feed back principle, the tracking system will move in order to make equal the received lights L_1 and L_2. Consequently, the system will be no more locked on the sun position during the disturbance. When the disturbance disappears, the system must return to its initial correct position.
For this simulation, the system is initially "pointed" in the south direction, (i.e. α_{ref} =0° or Vc=V_{cc}/2). And we set up L_0= 1000Lux. A disturbance is applied corresponding to a sudden reduction of 500 Lux on LDR1 during 1 second. Maximum deviation of α is around $\pi/4$ which corresponds logically to the point L2=500 Lux, on figure 19. α returns correctly to the initial position after the disturbance (Cf. figure 24).

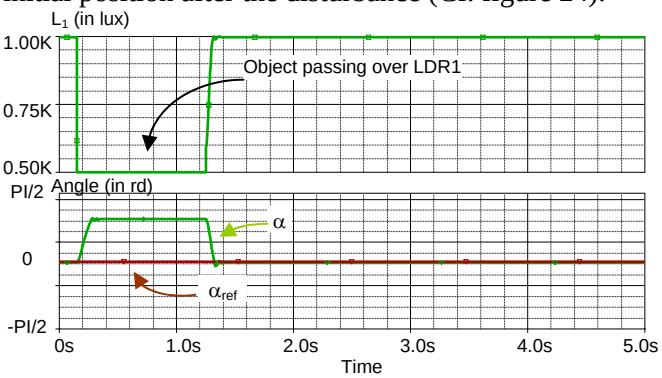

Figure 24: Closed loop transient response to a disturbance on D input.

5. Electronic design

The design uses only COTS components. The two LDR sensors (VT90N2 series or equivalent) are placed in a Wheatstone bridge. Output signals are subtracted using rail to rail OP amps LMC6482 to have the widest dynamic range. Difference V_{diff} is applied to the simple PID corrector (adjustable gain+ low pass RC filter). The resulting DC voltage value is converted linearly into a PWM signal, to control a classical Parallax (or equivalent) servomotor. This DC to PWM converter is based on a clever modified NE 555 circuit. Supply voltage comes through a LM7805 regulator +5V.

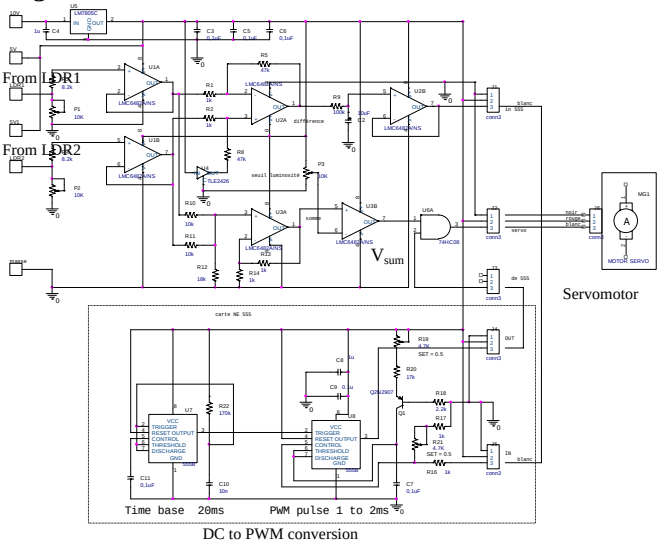

Figure 25: Electronic circuit schematic

6. Mechanical design

Figure 26 shows the final installation in the small scale house surroundings. Size of the small solar panel is 6cm x 5cm. Distance between LDR is 10cm.

Figure 26: small scale solar tracking system installation

7. Experiment

7.1 Static open loop measurement

As static and dynamic characteristics of servomotor were unknown (no manufacturer data), an open loop characterisation were performed to investigate its behaviour and to compare to simulation.
System was placed in a dark room in front of a single 75W spot light (1meter far) simulating the sun.

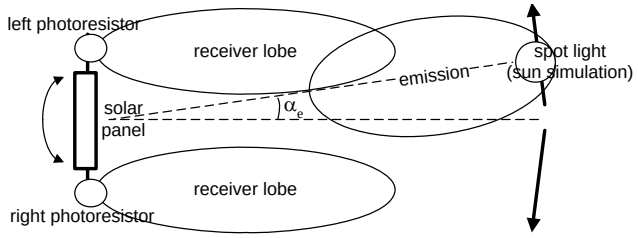

Figure 27: Static open loop characterisation

Experimental sensor static voltage difference V_{diff} and sum V_{sum} versus alignment angle α_e, are given in figure 28 and 29. Due to +5V V_{supply} single voltage supply operation, the sensor voltage difference V_{diff} is obviously centered on V_{supply} /2.

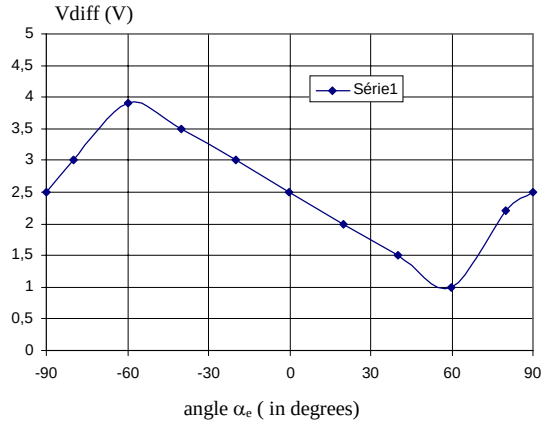

Figure 28: Sensor V_{diff} vs. angle α_e (in degrees)

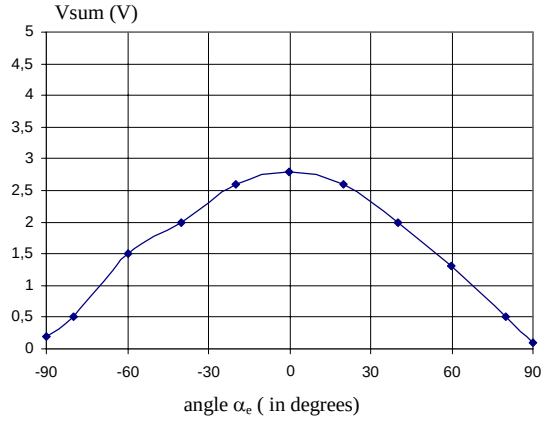

Figure 29: Sensor scaled voltage V_{sum}, vs. angle α_e (in degrees)

7.2 Dynamic open loop measurement

While rotation angle remains small (i.e. less than ±10°), the system response can be considered almost linear. That allows a classical analysis with an Agilent 33550 generator and digital oscilloscope Tek TDS 2004B. (Gain of P.I.D corrector not included).

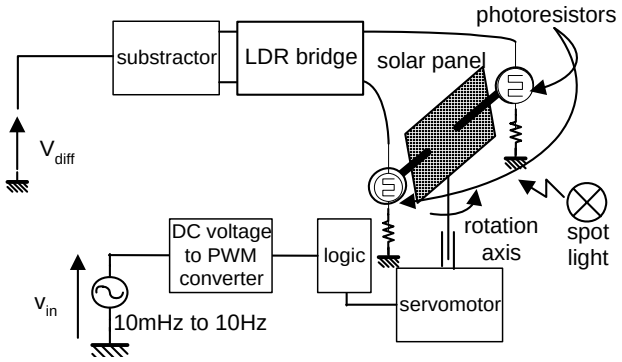

Figure 30: Open loop dynamic characterisation schematic

However, practical open loop response is extremely difficult to measure because of the ultra low working frequencies and output voltage low level. A realistic +/-5% error margin is indicated on figure 31.

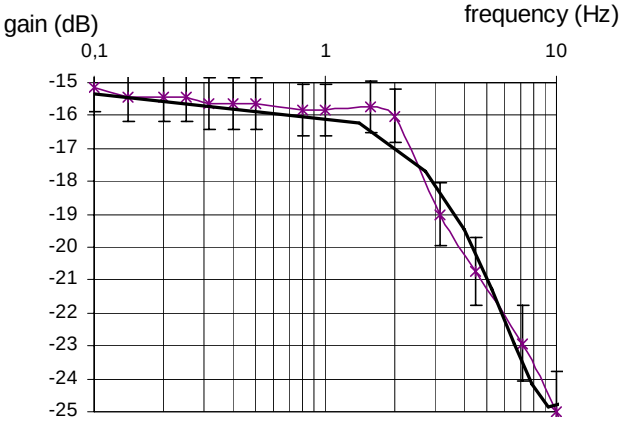

Figure 31: Experimental AC open loop gain V_{diff}/v_{in}

First cut-off frequency occurs at 1.58 Hz, (according to simulation's results).

7.3 Visual test and disturbance effects

Visual tests show that that tracking feed back loop works correctly. Validation of the system behaviour was done under various conditions (light source distance and intensity). By putting a shutter on one of LDR, we checked the effect of distance and the correct return to initial position when the shutter was removed. Finally, a small video clip was recorded to register the system behaviour.

A correct matching between global SPICE modelling, predicting simulations and experimental behaviour design is observed.

However, during indoor experimentation, small permanent oscillations of the servo occurred at one hundred hertz. These parasitic oscillations were identified as consequences of inherent flicker at 100Hz coming from ceiling fluorescent light. While "solar tracking" is an extremely slow system, no speed performances are needed for the feed back loop. Thus, the problem was solved by adding a low pass RC filter with a cut-off frequency of 10Hz without any impact on loop stability.

9. Future work

9.1 Modelling

The current Spice modelling gives satisfaction for predicting the performances of the small scale solar tracking system. However, it is possible to improve and refine some modelling blocks to obtain some more fine simulations.
Particularly, the servomotor modelling is not enough realists for a fine rotational movement representation. Some improvements have to be carried out.
Once done, the modelling will extended to a two axes solar tracking system.

9.2 Complementary study

A detailed study of LDR mismatching effect and non linearity impact will be performed as well as an improved electronic design. Results should be published in the near future. Stability at high light level will be investigated and an auto adaptative loop correction can be studied.

10. Conclusion

An equivalent modelling of a small scale one axis solar tracking system was presented. Mixed Spice modelling and electronic analogue designs were successfully validated by experimental tests.
This tracking system is now installed in our small scale green house modelling. And other accessories will be studied and designed to complete our Sustainable Development didactical tool. Lastly, from a pedagogical point of view, this study is now used for training the students during the feed back course, projects and practical lessons.

References:

[1] Ph. Dondon- P. Cassagne- M. Feugas- C.A. Bulucea- D.Rosca-V. Dondon- R. Charlet de Sauvage "*Concrete experience of collaboration between secondary school and university in a sustainable development project: design of a realistic small scale house to study electronic and thermal aspect of energy management.*" WSEAS Transactions on ENVIRONMENT and DEVELOPMENT Issue 10, Vol 7, oct 2011, ISSN: 1790-5079 p 225-235
[2] « *Choix d'un suiveur solaire* » http://www.energieplus-lesite.be/energieplus/page_16690.htm?reload
[3]http://www.exosun.fr/index.php
[4] P.J. Axaopoulos, K. Moutsopoulos, M.P. Theodoridis *« Solar Engineering Education* » Proceedings of the 8th WSEAS International Conference on Engineering Education, Corfu, Greece July 14-16, 2011
[5] Ph. Dondon « *radars à ultrasons* » web site : http://uuu.enseirb.fr/~dondon/PIC/autrapplication/RadardepoursuiteetdemesureUltrason.htm
[6] T. Bendib, B. Barkat, F. Djeffal, N. Hamia et A. Nidhal « *Commande automatique d'un système de poursuite solaire à deux axes à base d'un microcontroleur PIC16F84A »* Revue des Energies Renouvelables Vol. 11 N°4 (2008) 523 – 532
[7] M.D. Draou, B. Draoui, « *Etude, conception et expérimentation d'un système de contrôle pour système suiveur de soleil* » Revue des Energies Renouvelables Vol. 11 N°2 (2007) 229 – 238
[8] P.L. Milea, O. Oltu, M. Dragulinescu, M. Dascalu «*Optimizing solar panel energetic efficiency using an automatic tracking microdetector*» Proceedings of the WSEAS International Conference on Renewable Energy Sources, Arcachon, France, October 14-16, 2007
[9] P. BONNET « *Cours de Traitement d'Images* » Université des Sciences et Technologies de Lille, France, web site : www-lagis.univ-lille1.fr/~bonnet/image/imaphy.pdf
[11] E. Lemery « *Les photorésistances, technologies, propriétés et application* » Electronique application n°57 p 51-65
[12] F. Morain-Nicolier « *Cours Capteurs, chap 8. capteurs optiques* » URCA - IUT de Troyes Ge2i - S3 2005
[13]A. Dias Tavares1, M. Muramatsu2 «*Some Simple Experiments in Optics Using a Photo-Resistor*» International Journal on Hands-on Science ISSN (print): 1646-8937; (online): 1646-8945Vol. 1, n° 2, Dec 2008.